Multi-Agent System-Based Microgrid Protection Using Angular Variation: An Embedded Approach

F.A.S. Dizioli*, P.H.A. Barra†, T.S. Menezes*, V.A. Lacerda‡, D.V. Coury*, R.A.S. Fernandes†
* Department of Electrical and Computer Engineering, São Carlos School of Engineering
University of São Paulo, São Carlos, Brazil
† Department of Electrical Engineering, Federal University of São Carlos, São Carlos, Brazil
‡ Centre d'Innovació Tecnològica en Convertidors Estàtics i Accionaments
Universitat Politècnica de Catalunya (CITCEA-UPC), Barcelona, Spain

***Abstract* – This paper presents a new approach for protecting microgrids based on multi-agent systems and using the angular variation of currents. The multi-agent system was structured using a congregation organization with three agents: section agent, circuit breaker agent, and switch agent. In this proposal, section agents are located at the microgrid lines, obtaining the difference in current angles between the buses. Then, if a threshold is reached, it sends a trip signal to the circuit breaker agent. This agent is responsible for receiving the trip signals and determining the correct line to be isolated. Finally, the switch agent is responsible for monitoring the microgrid operating scenario and updating the adequate thresholds of the agents. The proposed method was assessed firstly using simulations in PSCAD. Next, the multi-agent strategy was embedded into a low-cost microcontroller unit and tested through hardware-in-the-loop (HIL) experiments using the Real-Time Digital Simulator (RTDS). The experimental and simulation results indicated the feasibility of the proposed method.**

***Keywords*: Hardware-in-the-loop, Microgrid, Multi-agent System, Power System Simulation, Protection.**

I. Introduction

DISTRIBUTED energy resources (DERs) continue to grow, especially considering their decreasing cost and the need to decarbonize electric power systems. At the distribution level, microgrids (MGs) help to integrate DERs into electric power grids, improving power quality, reliability, efficiency, electricity management, and other indicators [1], [2]. MGs can be addressed as local entities comprised of loads, lines, and DERs. Thus, MGs operate within a distribution network in a grid-connected manner or with the islanded operating mode [3]. It is essential to observe that MG islanding capability is one of their main advantages because when an undesired event occurs in the main grid, the MGs can efficiently maintain its operation.

Despite the advantages of MGs, some challenges remain in implementing them on a large scale, such as their protection [1], [4]. Note that in conventional distribution systems, the fault detection procedure (intrinsic to the online protection scheme) is usually based on the rise in the current magnitude. This conventional protection might not be adequate for MGs [5] due to some aspects: i) short-circuit currents can vary considerably, depending on the connection mode of the MG (grid-connected or islanded) or connection/disconnection of DERs; ii) there is a bidirectional power flow at some points of the MG, also depending on the status of DERs and connection of the lines; iii) the MG can operate in different topologies considering, for example, self-healing actions; and iv) some DERs can be intermittent and disconnected at any time.

From the above-mentioned challenges, a MG protection strategy should be reliable and sensitive in detecting faults and enabling fast fault clearance. Thus, many researchers have devoted efforts to proposing new strategies and schemes for protecting MGs. In [4], the authors presented a comprehensive survey on MG protection, showing the recent research advances and proving that more progress is required in this topic. It can be noticed that machine learning (ML)-based protection strategies have been proposed for fault diagnosis [6], [7] and [8], and more specifically, for MG protection [9], [10], [11], [12], [13], [14], [15], [16] and [17]. Despite the good performances of these approaches, the training stage and the large number of attributes to compose the algorithms can be highlighted as shortcomings.

More recently, strategies that use multi-agent systems (MAS) are considered promising in protecting MGs. In the literature, there are studies with compelling results using MAS, such as [18], [19], [20] and [21]. Nevertheless, some concerns must be addressed to improve the practicality of the MAS-based proposals. Major studies do not explore real-time tests, assessing the practical behavior of methods on the hardware level. External factors such as noise, filters, hardware and software limitations, and measurement errors in experimental trials can jeopardize the protection schemes' response. Another observed factor is the lack of diversification of simulation tests. In many studies, the assessment of the proposals is limited regarding the fault type, resistance values, fault locations, and operating scenarios of the MG.

In this context, this paper proposes a new approach to protect MGs using MAS. In this scheme, the agents obtain the angles of the currents at points of interest in the MG. Thus, from the variation of the angular differences, the MAS-based protection can properly detect faults. Firstly, the protection was evaluated through several computational simulations in

This work was support in part by the São Paulo Research Foudation (FAPESP) [Grant Number 2021/04872-9], The Brazilian National Council for Scientific and Technological Development (CNPq) [Grant Number 134179/2020-0], and Coordenação de Aperfeiçoamento de Pessoal de Nível Superior – Brazil (CAPES) [Finance Code 001].

Paper submitted to the International Conference on Power Systems Transients (IPST2023) in Thessaloniki, Greece, June 12-15, 2023.

PSCAD™/EMTDC™ software, considering diversified faulty scenarios. Then, the proposal was validated through hardware-in-the-loop (HIL) experiments. In this second stage, the agents were embedded into a Texas Instruments development board, and closed-loop experiments were conducted using the Real-Time Digital Simulator (RTDS). The overall MAS structure enables reliable fault detection and clearance concerning the MG.

The main contributions of this paper to advance the state-of-the-art in terms of MG protection are as follows:

1. The MAS-based approach uses a simple calculation of difference of current angles to detect faults.
2. The approach was embedded into a low-cost microcontroller unit (MCU), demonstrating its simplicity and applicability. Few studies evaluate their proposals at a hardware level.
3. The approach can be used for primary and backup MG protection, along with other strategies.

The remainder of this paper is organized as follows. Section II briefly presents the foundations of MAS. The proposed protection approach is presented in Section III. Then, Section IV addresses the simulation results, while Section V shows the HIL experimental results. Finally, Section VI draws the conclusions.

II. Multi-Agent Systems

In the context of computer science, an agent can be defined as a computer system implemented or conceptualized with some human characteristics. The intelligent agent is programmed to act within a specific environment (deterministic or stochastic). Thus, the agent can act to accomplish individual or collective objectives. Even though there is no consensus on the definition of an intelligent agent, in [22] the authors define that a computer program is an intelligent agent if it has the following features:

- autonomy – agent operates on its own, without external intervention;
- social ability – agent can communicate with other agents using some communication language;
- reactivity – agent notices changes in the environment and acts accordingly to these changes;
- pro-activeness – agent not only acts based on external stimuli, but also takes initiative to accomplish an objective.

MAS are systems with two or more agents. In the literature, there are some methods to organize the MAS. The most common organization is the hierarchical one, where communication between agents on the same level has to pass through the agent on the upper levels. The agents on the upper levels give the orders to the agents on the levels below. Another organization is the society, in which agents can participate or not, but if they do, they have to follow a set of internal rules. There are also agents organized in a congregation. In this organization, multiple agents are divided into specific functions which a single agent might not achieve alone. The mentioned organizations are illustrated in Fig. 1.

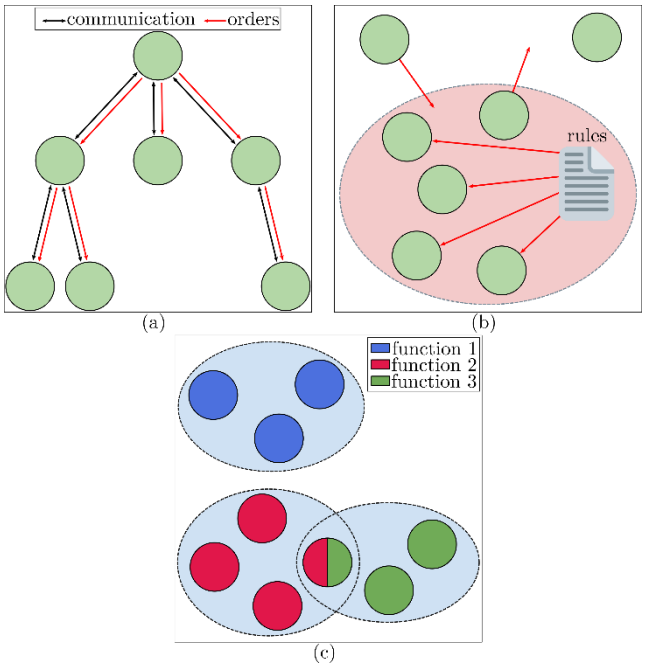

Fig. 1. Agents' organization: (a) hierarchical; (b) society and (c) congregation.

III. Proposed Protection Algorithm

In this paper, the MAS was structured using the congregation organization with three functions. The description of each function is presented next:

- Section agent – this monitors the difference of current angles at the ends of a line to decide if there is a fault on the monitored line. If there is, this agent sends a trip signal to the circuit breaker agent;
- Circuit breaker agent – based on the received trip signals and difference of current angles from the section agents, it determines what circuit breakers should actuate to isolate the fault;
- Switch agent – this tracks the state of the switch connecting the MG to the main supply, identifying if the MG is connected or islanded to properly select the detection thresholds used by the section agents.

A general overview of the proposed MAS protection scheme is presented in Fig. 2, which denotes how the agents operate.

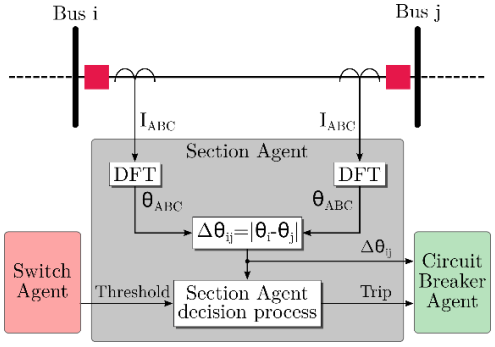

Fig. 2. Diagram of the proposed MAS protection scheme.

As shown in Fig. 2, the section agents are located at each line of the system. They calculate the difference of current

angles (Δθ) between two generic buses *i* and *j* at sample *k*, as presented in (1).

$$\Delta\theta_{ij,k} = |\theta_{i,k} - \theta_{j,k}|. \quad (1)$$

In Eq. (1) and Fig. 2, it can be observed that the proposed scheme has an approach based on differential relays, requiring only phase angles instead of the full current phasors.

If Δθ variation is above a threshold and below 90◦ for three consecutive samples, the section agent sends a trip signal to the circuit breaker agent. The complete decision process for the section agent is shown in Fig. 3.

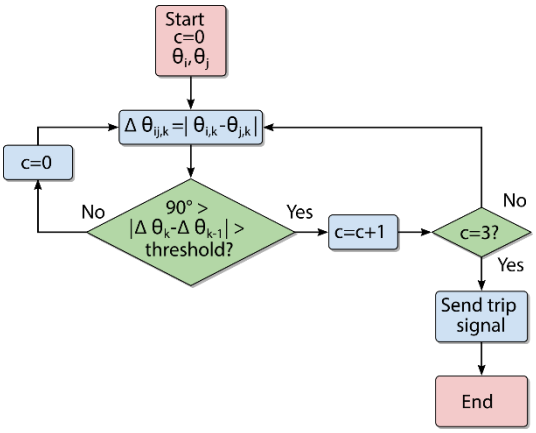

Fig. 3. Flowchart of the section agent decision process.

The threshold is obtained by simulating a high resistance (50 Ω) single-phase fault and choosing the highest post-fault variation (Δθ), which leads to this fault detection. Thus, the thresholds are defined using the value obtained in this analysis (3.5° for the connected MG and 2.5° for the islanded MG). Note that the upper limit of 90° exists to prevent the protection from acting under sudden variation of Δθ. The main cause of this variation is the phasor estimation limiting the phase angle between ±180°. For example, when the phase angle is close to 180° and suffers a slight rise, it shifts over to -180°, which might cause a difference of up to 360°.

Then, the circuit breaker agents receive Δθ and the trip signal information from the section agents. If a circuit breaker agent simultaneously receives trip signals from more than one section agent, it proceeds to compare the Δθ information from these agents and trips the circuit breakers in the line with the highest absolute value of Δθ. Fig. 4 shows the decision process for the circuit breaker agent. It is appropriate to clarify that the circuit breaker agent is a computational entity different from the physical circuit breaker. This agent monitors the trip signals from section agents and is responsible for deciding and sending trip signals to the appropriate physical circuit breakers.

Finally, the switch agent continuously monitors the state of the switch connecting the MG to the main supply. This agent selects the appropriate threshold value used by the section agent according to the MG status. Thus, this agent is responsible for providing adaptability to the MAS-based protection. In this paper, only three-pole-operated circuit breakers were considered. Moreover, the fault clearance was not dependent on the fault type classification. Then, a strategy for classifying faults was not required here for protection purposes. This feature could be added in future work, as it can be helpful for other applications, such as fault location.

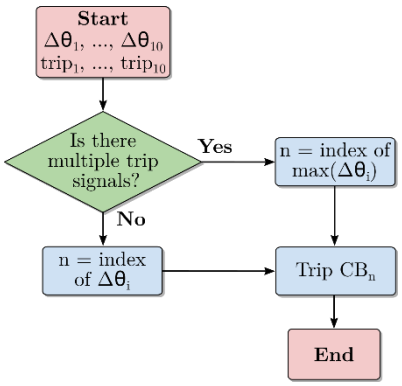

Fig. 4. Flowchart of the circuit breaker agent decision process.

It is important to note that each agent acquires local current measurements. Therefore, it is possible to check if the communication is continuous, ensuring that the protection works correctly. If any communication failure is detected, the agent is able to work independently, i.e., without communication, by a traditional overcurrent scheme. Furthermore, this backup protection can be coordinated due to the low response time of the proposed method. Finally, concerning the current technology, it is worth mentioning that there are some commercial devices with phase angle accuracy that enable the practicality of this proposal. These devices and upcoming developments ensure that protection schemes are more accurate.

IV. Simulation Results

The analyses of the proposed protection algorithm were performed using a test MG based on the European medium-voltage distribution network benchmark from CIGRE [24], as depicted in Fig. 5. Note from this figure that the MG has a delimited region, ranging from buses 3 to 11. Moreover, a circuit breaker (CB1) is responsible for the connection/disconnection of the MG to the main grid. In this MG, a 5 MVA synchronous generator is connected to bus 5, with parameters from [25]. When the MG operates connected to the main grid (grid-connected mode), the generator operates in active-reactive power (PQ) control mode, while in islanded mode, the generator operates in frequency-voltage (fV) control mode. Finally, Fig. 5 shows the section and switch agents.

In the first part, several simulations were carried out using the PSCAD™/EMTDC™ software. In these simulations, different operating conditions of the MG were considered for testing the proposed approach. Some parameters were changed in the simulations through an interface between PSCAD™/EMTDC™ and Python, generating all the simulations. These parameters are listed next:

- Fault types – single-phase-to-ground fault (involving phase A and ground), phase-to-phase fault (involving phases B and C), double-phase-to-ground fault

(involving phases A and C, and ground), and three-phase fault (involving phases A, B, and C);

- Fault resistances – 0 Ω, 10 Ω, 20 Ω, 30 Ω, 40 Ω, and 50Ω;
- Fault locations – at 25%, 50%, and 75% of lines 3-4, 4-5, 5-6, 3-8, 8-7, 8-9, 9-10, and 10-11;
- Microgrid operation mode – connected and islanded.

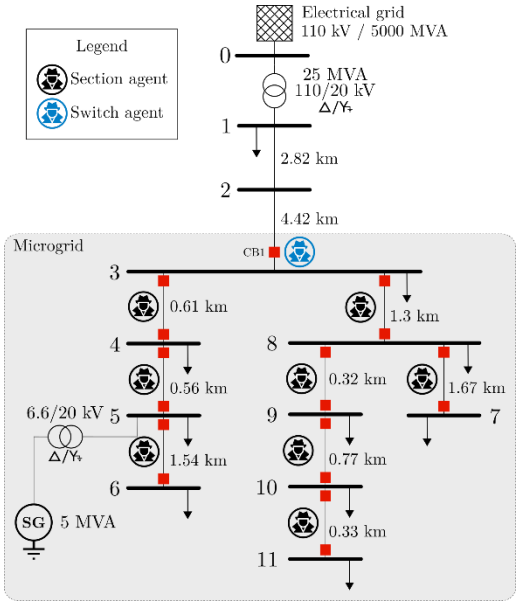

Fig. 5. Test system with all the electrical connections and agents' locations.

Combining all these parameters derived 576 fault cases for each operation mode (connected and islanded), thus resulting in 1,152 fault situations. Concerning the mentioned fault types, it is important to observe that the tested MG is balanced, making the analyzed types representative. The angles used by the section agents were obtained from the fundamental frequency component of the phase currents using the fast Fourier transform with 64 samples/cycle. In the next section, the detection procedure will be illustrated for two specific cases. Then, the final results of the proposed approach will be presented considering all the simulations.

A. Case 1 – MG in islanded mode

Firstly, a particular fault case was analyzed to illustrate the fault detection procedure. This one is a three-phase solid fault in the middle of line 3-4, considering the islanded MG. Even in the islanded mode, the three-phase faults tend to be easier to detect, as they cause more significant perturbation on all phases of the MG. Fig. 6 shows the behavior of line 3-4 section agent during the fault. It can be observed that the circuit breaker agent generated the tripping signal after three consecutive variations of Δθ higher than the considered threshold (2.5°). This operation occurred approximately 2 ms after the fault inception at 1.5 seconds.

B. Case 2 – MG in grid-connected mode

Secondly, another fault from the simulations was analyzed. In this case, a single-phase-to-ground (involving phase A and ground) with fault resistance of 50 Ω was simulated at line 3-4, considering the grid-connected mode. This fault is more challenging to detect than the first case, considering its type and fault resistance. Fig. 7 depicts the section agent behavior, where the angle difference variations can be observed. It can be noted that the agent only detects significant variations of Δθ for phase A, taking more time to detect the three consecutive variations above the threshold (3.5°). Nevertheless, the agent rapidly detected the fault in less than one cycle, 9 ms after the fault inception at 1.5 seconds.

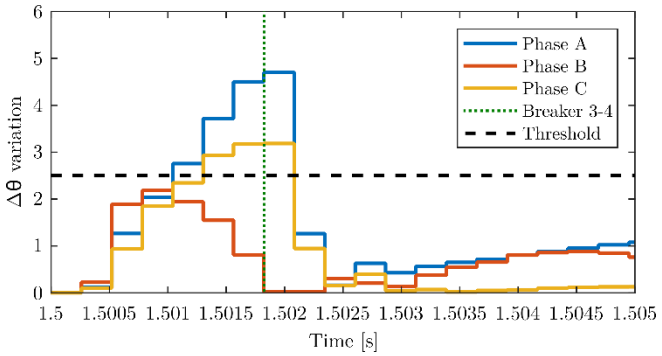

Fig. 6. Angle difference variation in line 3-4 for a solid three-phase fault with the MG islanded.

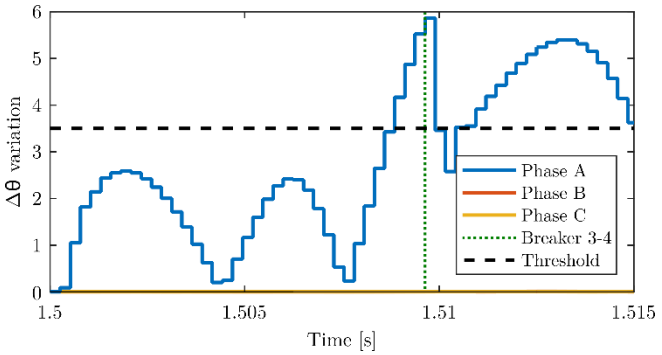

Fig. 7. Angle difference variation in line 3-4 for a 50 Ω single-phase fault with the MG connected.

C. General performance of the proposed approach

Concerning the performance of the proposed approach for all the simulations, Tables I and II show the obtained accuracies considering the different fault types and resistances. It can be observed that the MAS-based approach was able to detect all the fault types with resistances up to 30 Ω, disregarding the MG operating mode (grid-connected or islanded). For faults with more than 30 Ω, the proposed approach tended to be less accurate, but the accuracy values continued to be high. Moreover, it can be observed that the proposed approach correctly detected all the three-phase faults, which are the most harmful to the MG, regardless of its operating mode. Finally, the resulting average accuracies considering the grid-connected and islanded modes were 97.9% and 96.0%, respectively, implying in a final average of 97.0% regarding all the scenarios.

The simulations were also analyzed by adding noise, modeled as a White Gaussian noise with a signal-to-noise ratio of 30 dB and 50 dB, respectively. Nonetheless, the noise did

not affect the performance of the proposed method, which obtained the same accuracies shown in Tables I and II. Since the Fourier Transform acted as a filter, the effect of noise was mitigated after data acquisition.

TABLE I
PERCENTAGE OF CORRECT FAULT DETECTION FOR FAULT TYPE AND RESISTANCE IN GRID-CONNECTED MODE

		Fault type				Total
		Type I[(1)]	Type II[(2)]	Type III[(3)]	Type IV[(4)]	
Fault resistance [Ω]	0	100.0%	100.0%	100.0%	100.0%	100.0%
	10	100.0%	100.0%	100.0%	100.0%	100.0%
	20	100.0%	100.0%	100.0%	100.0%	100.0%
	30	100.0%	100.0%	100.0%	100.0%	100.0%
	40	87.5%	100.0%	87.5%	100.0%	93.8%
	50	87.5%	100.0%	87.5%	100.0%	93.8%
Total		95.8%	100.0%	95.8%	100.0%	**97.9%**

(1) single-phase-to-ground fault; (2) phase-to-phase fault; (3) double-phase-to-ground fault; and (4) three-phase fault.

TABLE II
PERCENTAGE OF CORRECT FAULT DETECTION FOR FAULT TYPE AND RESISTANCE IN ISLANDED MODE

		Fault type				Total
		Type I[(1)]	Type II[(2)]	Type III[(3)]	Type IV[(4)]	
Fault resistance [Ω]	0	100.0%	100.0%	100.0%	100.0%	100.0%
	10	100.0%	100.0%	100.0%	100.0%	100.0%
	20	100.0%	100.0%	100.0%	100.0%	100.0%
	30	100.0%	100.0%	100.0%	100.0%	100.0%
	40	75.0%	100.0%	87.5%	100.0%	90.6%
	50	66.7%	100.0%	75.0%	100.0%	95.4%
Total		90.3%	100.0%	93.8%	100.0%	**96.0%**

(1) single-phase-to-ground fault; (2) phase-to-phase fault; (3) double-phase-to-ground fault; and (4) three-phase fault.

A compelling feature of a protection system is associated with a rapid clearing time of the faults. In the proposed approach, relatively low response times were obtained. Table III presents information about the protection's response times, showing some statistical indicators. It can be observed that the maximum clearing time was 10.16 ms, while 75% of the faults were cleared within 1.82 ms (third quartile). In the islanded mode, the maximum clearing time was 2.60 ms and the average clearing time was 1.61 ms. Note that the response time of the MAS-based protection can be delayed if needed, allowing it to perform a primary or backup function with other strategies.

Finally, it can be observed that the proposed approach overcomes some conventional strategies for MG protection. In [25], it can be seen that the accuracy of an overcurrent relay in protecting MGs is 61.25%, while the accuracy of a current differential relay is 88.22%. In this paper, the MAS-based protection presented an average accuracy of 93.4%. These results were not assessed for the same MG, but they provide a general overview of the different approaches concerning their accuracy.

TABLE III
STATISTICAL ANALYSIS OF PROTECTION'S RESPONSE TIMES

Detection time	Islanded	Connected	General
Average	1.61 ms	1.83 ms	1.72 ms
Standard deviation	0.34 ms	1.53 ms	1.12 ms
Minimum	1.04 ms	1.04 ms	1.04 ms
Maximum	2.60 ms	10.16 ms	10.16 ms
First quartile	1.30 ms	1.30 ms	1.30 ms
Median	1.56 ms	1.56 ms	1.56 ms
Third quartile	1.82 ms	1.56 ms	1.82 ms

V. HARDWARE-IN-THE-LOOP RESULTS

Real-time experiments were performed to evaluate the proposed strategy implemented in hardware. The section agent was embedded in an MCU, which was a C2000 Delfino F28379D Launchpad development board [26], designed by Texas Instruments. A set of closed-loop analyses were conducted using the RTDS platform [27].

The fault currents previously simulated were appropriately normalized to be generated using the RSCAD/RTDS as analog voltage signals in a range of 0 and 3 V, which is the input range for the MCU. Then, the signals passed through analog low-pass filters with a cut-off frequency of 360 Hz, to mitigate the influence of noise. Finally, the MCU acquires the analog signals using six 12-bit analog-to-digital converter modules with a resolution of 4,096 levels and a sampling frequency of 3,840 Hz (64 samples/cycle). After these steps, the MCU can perform all the decision processes of the section agent. If a fault is detected, the tripping signals for each phase and the final trip are sent to the RTDS, closing the loop. The laboratory setup for the hardware tests is presented in Fig. 8.

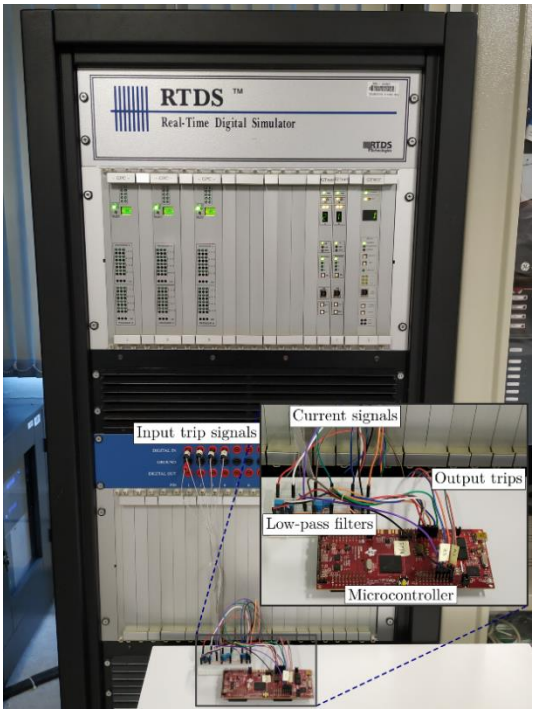

Fig. 8. Laboratory setup for the hardware tests.

The Simulink Coder [28], version 2019b, was used for embedding the algorithms into the MCU. Some parts of the section agent algorithm were constructed using C language, including the discrete Fourier transform and the agent's decision core. Other parts of the section agent were designed through Simulink blocks, which were later converted into C code by the Simulink Coder in the embedding stage. In this step, a time delay of 5.2 ms (20 samples) was considered in the final trip from the section agents. This consideration aims to represent the time of exchanged messages between the agents, according to the IEC-61850 standard. This standard makes it possible to obtain rapid horizontal communication, with a time to exchange messages between the agents in around 0.25 cycle (4-5 ms) [29], [20].

For the real-time experiments, some faults from all the 1,152 cases were chosen for testing. These cases are faults at line 3-4, considering the importance of this line for the operation of the MG. Thus, the section agent 3-4 (*Ag#3-4*) was chosen for this analysis. The fault cases used for the real-time tests are as follows:

- Test 1 – 20 Ω three-phase fault at line 3-4 with MG connected;
- Test 2 – 20 Ω single-phase-to-ground (involving phase A and ground) fault at line 3-4 with MG connected;
- Test 3 – 20 Ω three-phase fault at line 3-4 with MG islanded;
- Test 4 – 20 Ω single-phase-to-ground (involving phase A and ground) fault at line 3-4 with MG islanded;
- Test 5 – Solid three-phase fault at line 3-8 with MG connected (external fault for the *Ag#3-4*);

Tests 1 to 4 comprise faults on line 3-4, and the section agent, *Ag#3-4*, must isolate the fault. Conversely, Test 5 consists of an external fault on line 3-8, and the section agent *Ag#3-4* should not detect this fault, as it occurs out of this protection zone. The input signals and output trip signals of the section agent for the real-time Test 1 are illustrated in Fig. 9.

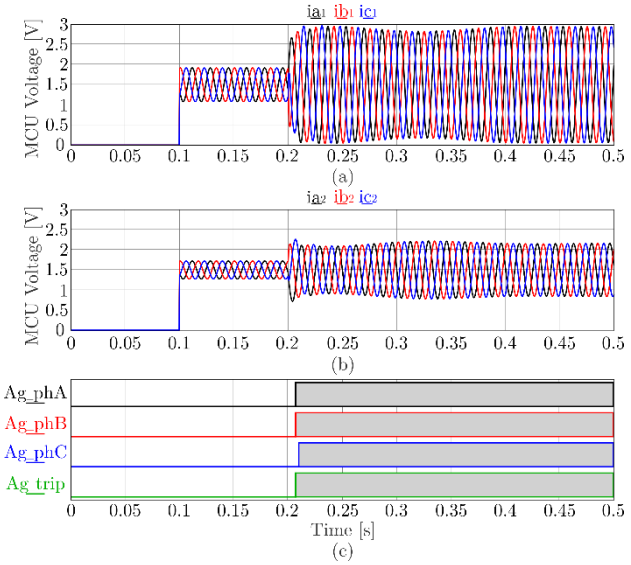

Fig. 9. Normalized current signals measured at (a) bus 3, (b) bus 4, and (c) the output trip signals of the section agent *Ag#3-4* for the real-time test 1.

As shown in Fig. 9, the proposed protection scheme correctly detected the fault from Test 1. The section agent presented trip signals for all phases, which ensures the fault detection for this test. Fig. 10 presents the section agent response for Test 2. Once more, the section agent correctly detected the single-phase fault with a fast resulting trip signal for phase A.

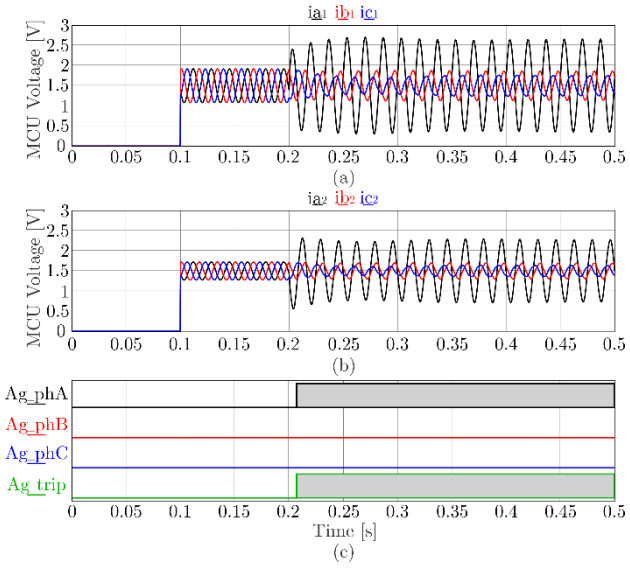

Fig. 10. Normalized current signals measured at (a) bus 3, (b) bus 4, and (c) the output trip signals of the section agent *Ag#3-4* for the real-time test 2.

Fig. 11 depicts a test with the MG islanded. In this particular case, note that the methods based on the rise in the current magnitude might not detect the fault as, after the fault inception, the current on bus 3 (Fig. 11a) drops slightly. Nevertheless, the proposed protection properly detected the fault with resulting trips for phases A and C within the time window shown. In Test 4 (Fig. 12), the proposed protection detected the fault once more, with a fast trip for phase A.

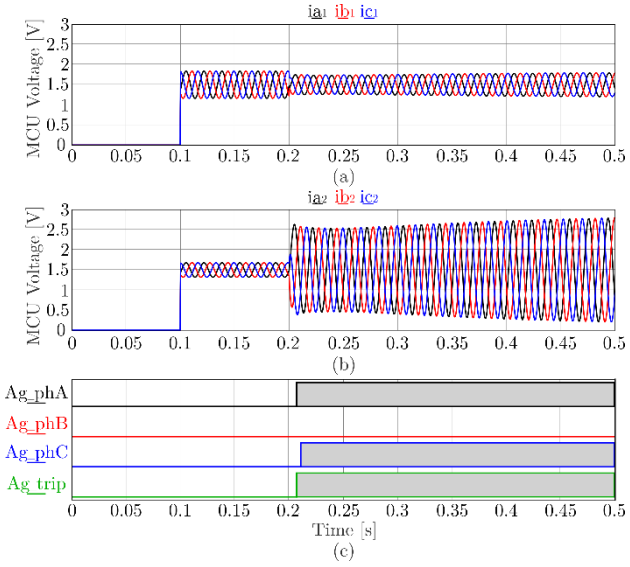

Fig. 11. Normalized current signals measured at (a) bus 3, (b) bus 4, and (c) the output trip signals of the section agent *Ag#3-4* for the real-time test 3.

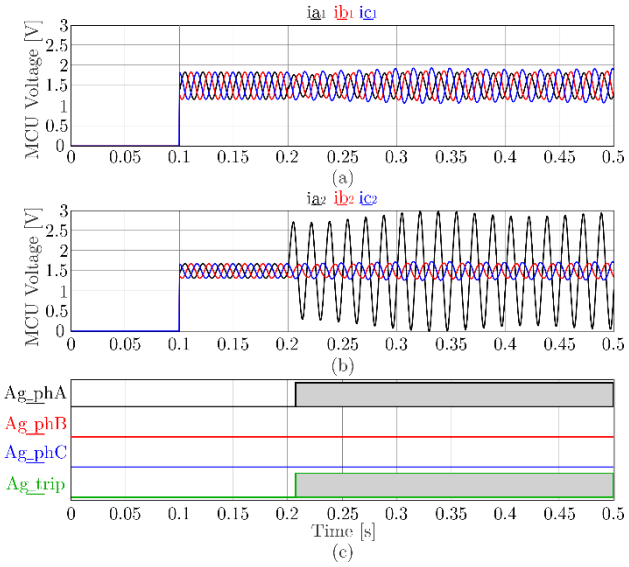

Fig. 12. Normalized current signals measured at (a) bus 3, (b) bus 4, and (c) the output trip signals of the section agent *Ag#3-4* for the real-time test 4.

Finally, Fig. 13 shows the last response of the proposed MAS-based protection for Test 5, which is a case of an external fault for the section agent *Ag#3-4*. Despite being an external fault, the fault currents also flow throughout the line protected by *Ag#3-4*. However, although there were substantial changes in the current signals, the section agent operated properly, not detecting this external fault.

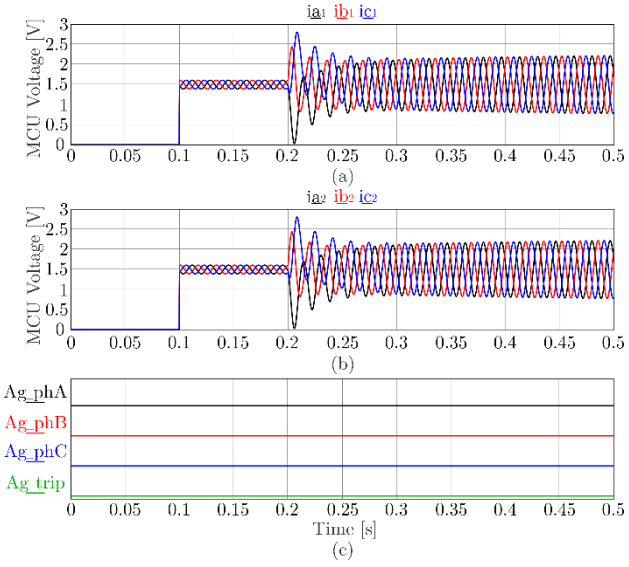

Fig. 13. Normalized current signals measured on (a) bus 3, (b) bus 4, and (c) the output trip signals of the section agent *Ag#3-4* for the real-time test 5.

The trip times for the five tests analyzed in the real-time experiments are presented in Table IV, where the cases in which no trip occurred were represented by "–". It can be observed that the obtained times from real-time experiments were very similar to the simulated ones. Moreover, in the real-time experiments, delays resulting from hardware elements and the considered time delay for the communication between the agents exist. Despite these aspects, the MAS-based protection continued to have a fast response. Additionally, considering the conducted real-time experiments, the proposed section agent detection process has shown to be reliable and selective to detect only faults within its detection zone.

TABLE IV
TRIP TIMES FOR REAL-TIME EXPERIMENTS

Trip time	Phase A	Phase B	Phase C	General
Case 1	7.28 ms	7.80 ms	9.88 ms	7.28 ms
Case 2	7.02 ms	–	–	7.02 ms
Case 3	7.54 ms	–	11.18 ms	7.54 ms
Case 4	7.28 ms	–	–	7.28 ms
Case 5	–	–	–	–

Finally, it is worth noting that the HIL tests were performed with a high background noise level. Thus, it also shows that noise does not affect the performance of the proposed protection scheme.

VI. CONCLUSIONS

In this paper, a new protection scheme for MGs was proposed. The method uses an MAS organized in conjunction with different functions to accomplish the desired decision process. Simulations were conducted considering 1,152 faults and different operating modes of MG. The simulation results showed that the proposed MAS-based protection scheme is promising, presenting good accuracy and a fast response time. Furthermore, a section agent was embedded into a MCU and real-time experiments were performed using RTDS. In the real-time tests, the MAS-based approach maintained a fast response and selectivity. Finally, it should be highlighted that few studies show real-time experiments to assess their proposed strategies. Nevertheless, this type of test is highly important to ensure the safety and reliability of the protection schemes for a future real-world implementation. Future work could address an additional feature of fault type classification, supporting other applications, such as fault location. Another promising sequence to this work is to explore and extend the proposed protection scheme for multi-microgrid systems. Finally, exploring the economic and stability aspects of hardware devices required in this research is recommended.

VII. ACKNOWLEDGMENTS

The authors would like to thank the São Carlos School of Engineering, University of São Paulo, Brazil for the facilities provided.

REFERENCES

[1] M. A. Hossain, H. R. Pota, M. J. Hossain, and F. Blaabjerg, "Evolution of microgrids with converter-interfaced generations: Challenges and opportunities," International Journal of Electrical Power & Energy Systems, vol. 109, pp. 160–186, 2019.

[2] W. Ajaz and D. Bernell, "California's adoption of microgrids: A tale of symbiotic regimes and energy transitions," Renewable and Sustainable Energy Reviews, vol. 138, p. 110568, 2021.

[3] N. Hatziargyriou, H. Asano, R. Iravani, and C. Marnay, "Microgrids," IEEE Power and Energy Magazine, vol. 5, no. 4, pp. 78–94, 2007.

[4] P. H. A. Barra, D. V. Coury, and R. A. S. Fernandes, "A survey on adaptive protection of microgrids and distribution systems with distributed generators," Renewable and Sustainable Energy Reviews, vol. 118, p. 109524, 2020.

[5] J. Reilly and S. M. Venkata, “Microgrid protection: Its complexities & requirements [Guest Editorial],” IEEE Power and Energy Magazine, vol. 19, no. 3, pp. 14–19, 2021.
[6] J. Wang, S. Gao, L. Yu, D. Zhang, C. Xie, K. Chen, and L. Kou, “Data-driven lightning-related failure risk prediction of overhead contact lines based on bayesian network with spatiotemporal fragility model,” Reliability Engineering System Safety, vol. 231, p. 109016, 2023.
[7] L. Kou, C. Liu, G.-w. Cai, J.-n. Zhou, and Q.-d. Yuan, “Data-driven design of fault diagnosis for three-phase PWM rectifier using random forests technique with transient synthetic features,” IET Power Electronics, vol. 13, no. 16, pp. 3571–3579, 2020.
[8] Y. Zhou, Y. Sai, and L. Yan, “An improved extension neural network methodology for fault diagnosis of complex electromechanical system,” International Journal of Bio-Inspired Computation, vol. 18, no. 4, pp. 250–258, 2021.
[9] H. Lin, K. Sun, Z.-H. Tan, C. Liu, J. M. Guerrero, and J. C. Vasquez, “Adaptive protection combined with machine learning for microgrids,” IET Generation, Transmission & Distribution, vol. 13, no. 6, pp. 770–779, 2019.
[10] S. B. A. Bukhari, C.-H. Kim, K. K. Mehmood, R. Haider, and M. Saeed Uz Zaman, “Convolutional neural network-based intelligent protection strategy for microgrids,” IET Generation, Transmission & Distribution, vol. 14, no. 7, pp. 1177–1185, 2020.
[11] B. K. Chaitanya, A. Yadav, and M. Pazoki, “Wide area monitoring and protection of microgrid with DGs using modular artificial neural networks,” Neural Computing and Applications, vol. 32, pp. 2125–2139, 2020.
[12] Y.-Y. Hong, Y.-H. Wei, Y.-R. Chang, Y.-D. Lee, and P.-W. Liu, “Fault detection and location by static switches in microgrids using wavelet transform and adaptive network-based fuzzy inference system,” Energies, vol. 7, no. 4, pp. 2658–2675, 2014.
[13] S. Kar and S. R. Samantaray, “A fuzzy rule base approach for intelligent protection of microgrids,” Electric Power Components and Systems, vol. 43, no. 18, pp. 2082–2093, 2015.
[14] M. Singh and P. Basak, “Identification and nature detection of series and shunt faults in types I, III and IV wind turbines and PV integrated hybrid microgrid with a fuzzy logic-based adaptive protection scheme,” IET Gen., Transm. & Distrib., vol. 14, no. 22, pp. 4989–4999, 2020.
[15] S. A. Hosseini, H. A. Abyaneh, S. H. H. Sadeghi, R. Eslami, and F. Razavi, “A decision-tree scheme for responding to uncertainties in microgrid protection coordination,” Electric Power Components and Systems, vol. 46, no. 1, pp. 69–82, 2018.
[16] I. Sepehrirad, R. Ebrahimi, E. Alibeiki, and S. Ranjbar, “Intelligent differential protection scheme for controlled islanding of microgrids based on decision tree technique,” Journal of Control, Automation and Electrical Systems, vol. 31, no. 5, pp. 1233–1250, 2020.
[17] S. Ranjbar, A. R. Farsa, and S. Jamali, “Voltage-based protection of microgrids using decision tree algorithms,” International Transactions on Electrical Energy Systems, vol. 30, no. 4, p. e12274, 2020.
[18] M. H. Cintuglu, T. Ma, and O. A. Mohammed, “Protection of autonomous microgrids using agent-based distributed communication,” IEEE Transactions on Power Delivery, vol. 32, no. 1, pp. 351–360, 2017
[19] S. A. Ananda, J.-C. Gu, M.-T. Yang, J.-M. Wang, J.-D. Chen, Y.-R. Chang, Y.-D. Lee, C.-M. Chan, and C.-H. Hsu, “Multi-agent system fault protection with topology identification in microgrids,” Energies, vol. 10, no. 1, 2017.
[20] A. Kiani, B. Fani, and G. Shahgholian, “A multi-agent solution to multi-thread protection of dg-dominated distribution networks,” Int. Journal of Electrical Power & Energy Systems, vol. 130, p. 106921, 2021.
[21] F. B. dos Reis, J. O. C. Pinto, F. S. dos Reis, D. Issicaba, and J. G. Rolim, “Multi-agent dual strategy based adaptive protection for microgrids,” Sustainable Energy, Grids and Networks, vol. 27, p. 100501, 2021.
[22] M. Wooldridge and N. R. Jennings, “Intelligent agents: Theory and practice,” The knowledge engineering review, vol. 10, no. 2, pp. 115–152, 1995.
[23] CIGRE Task Force C6.04, “Benchmark systems for network integration of renewable and distributed energy resources,” 2014, Technical Brochure 575.
[24] F. A. Moura, J. R. Camacho, M. L. Chaves, and G. C. Guimarães, “Independent power producer parallel operation modeling in transient network simulations for interconnected distributed generation studies,” Electric Power Systems Research, vol. 80, no. 2, pp. 161 – 167, 2010.
[25] M. Mishra and P. K. Rout, “Detection and classification of micro-grid faults based on HHT and machine learning techniques,” IET Generation, Transmission & Distribution, vol. 12, no. 2, pp. 388–397, 2018.
[26] Texas Instruments, TMS320F2837xD Dual-Core Microcontrollers Datasheet (Rev. O), (accessed February 17, 2023), available at https://www.ti.com/product/TMS320F28379D.
[27] RTDS Technologies, (accessed February 17, 2023), available at https://www.rtds.com/about-rtds-technologies/.
[28] Simulink Coder, (accessed February 17, 2023), available at https://www.mathworks.com/products/simulink-coder.html.
[29] Z. Liu, C. Su, H. K. Høidalen, and Z. Chen, “A multiagent system-based protection and control scheme for distribution system with distributed-generation integration,” IEEE Transactions on Power Delivery, vol. 32, no. 1, pp. 536–545, 2017.